AAS 05-398

Gravity-Assist Trajectories to Jupiter Using Nuclear Electric Propulsion

Daniel W. Parcher[*] and Jon A. Sims[ϒ]

This paper examines optimal low-thrust gravity-assist trajectories to Jupiter using nuclear electric propulsion. Three different Venus-Earth Gravity Assist (VEGA) types are presented and compared to other gravity-assist trajectories using combinations of Earth, Venus, and Mars. Families of solutions for a given gravity-assist combination are differentiated by the approximate transfer resonance or number of heliocentric revolutions between flybys and by the flyby types. Trajectories that minimize initial injection energy by using low resonance transfers or additional heliocentric revolutions on the first leg of the trajectory offer the most delivered mass given sufficient flight time. Trajectory families that use only Earth gravity assists offer the most delivered mass at most flight times examined, and are available frequently with little variation in performance. However, at least one of the VEGA trajectory types is among the top performers at all of the flight times considered.

INTRODUCTION

The use of planetary gravity assists is a proven technique to improve the performance of interplanetary trajectories as exemplified by the Voyager, Galileo, and Cassini missions. Another proven technique for enhancing the performance of space missions is the use of highly efficient electric propulsion systems. Electric propulsion can be used to increase the mass delivered to the destination and/or reduce the trip time over typical chemical propulsion systems.[1,2] This technology has been demonstrated on the Deep Space 1 mission[3] – part of NASA's New Millennium Program to validate technologies which can lower the cost and risk and enhance the performance of future missions. With the successful demonstration on Deep Space 1, future missions can consider electric propulsion as a viable propulsion option. The combination of electric propulsion systems with gravity-assists trajectories can enable missions that would otherwise be impractical to execute.

Solar powered electric propulsion systems suffer substantial power loss as the spacecraft travels farther from the Sun, making nuclear powered electric propulsion a natural choice for trajectories that require substantial thrusting in the outer solar system since the nuclear power source does not diminish with increased solar distance. Several gravity-assist families that use nuclear electric propulsion to rendezvous with Jupiter have been presented previously including Mars gravity-assist families[4,5], single and double

[*] Member of the Engineering Staff, Guidance Navigation and Control Section, Jet Propulsion Laboratory, California Institute of Technology, Mail Stop 230-205, 4800 Oak Grove Drive, Pasadena, California 91109-8099. E-mail: Daniel.W.Parcher@jpl.nasa.gov. Phone: (818) 393-0457, Fax: (818) 393-4215.

[ϒ] Technical Manager, Guidance Navigation and Control Section, Jet Propulsion Laboratory, California Institute of Technology, Mail Stop 301-140L, 4800 Oak Grove Drive, Pasadena, California 91109-8099. E-mail: Jon.A.Sims@jpl.nasa.gov. Phone: (818) 354-0313, Fax: (818) 393-6388.

Venus gravity-assist families[5], and single and double Earth gravity-assist families[6] . This paper expands upon that work to include Venus-Earth gravity assists (VEGAs) and compare them to the previous results.

APPROACH

The preliminary design software used in this study to discover and analyze trajectories is based on a technique presented by Sims and Flanagan[7]. It uses a direct optimization method and models the thrust as small impulses. The starting and ending bodies (Earth and Jupiter, in this case) are treated as massless and the gravity assists are modeled as instantaneous changes in the direction of the $\mathbf{V}_\infty$ (hyperbolic relative velocity vector). The optimization objective for all of the trajectories presented is the maximization of the final mass of the spacecraft.

The maximum power available to the propulsion system is assumed to be fixed at 95 kW. The thrusters are modeled with a specific impulse of 6000 s and an efficiency of 70%. These parameters yield a maximum thrust of 2.26 N with a mass flow rate of 3.84×10^{-5} kg/s and are consistent with those used in References 5 and 6 so that the results can be compared directly. The software can choose whether or not to thrust at any point in time, the level of the thrust up to the maximum, and the direction of thrust.

The trajectories presented are injected to a positive energy with respect to Earth. The launch vehicle used for these trajectories has three times the capability of the Delta IV Heavy. The performance curve for this launch vehicle is illustrated in Figure 1, which shows the relationship between injection C_3 (defined as the square of departure V_∞ vector magnitude) and injected mass. In each of the trajectories presented, the injection V_∞ will be optimized in both direction and magnitude in order to maximize the final mass at Jupiter.

The performance curve in Figure 1 shows that injected mass is reduced substantially as the injection C_3 is increased. This relationship effectively penalizes trajectories that require higher injection C_3 values and provides the optimizer with an incentive to reduce C_3.

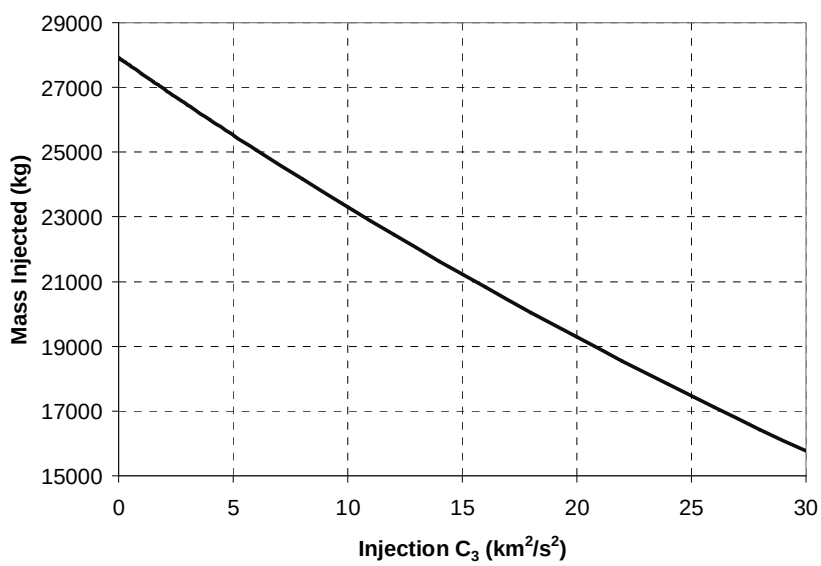

Figure 1 Launch Vehicle Capability Model

DIRECT TRANSFERS

Mass optimal direct Earth-to-Jupiter transfer performance for the assumptions outlined in the Approach section has been documented in Reference 5 and is shown here in Figure 2.* The data plotted in this figure was generated by parametrically varying flight time and reoptimizing the trajectory at each new flight time.

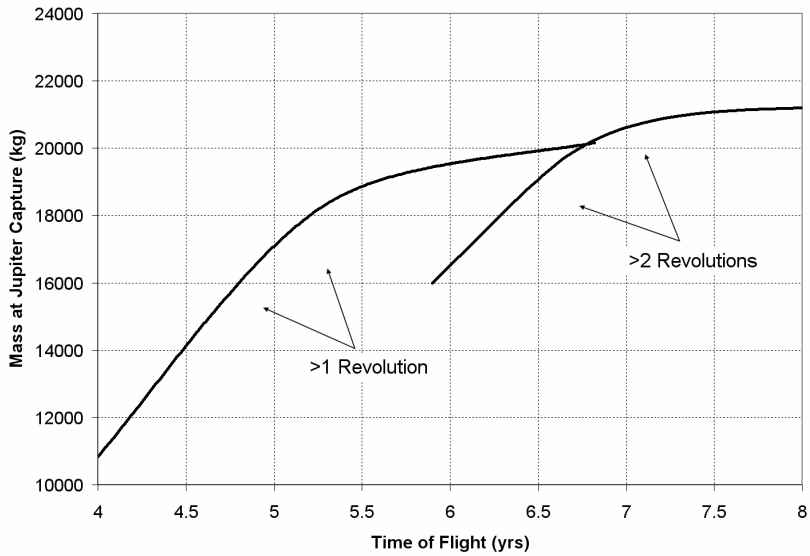

Figure 2 Direct Earth to Jupiter Transfers – Delivered Mass vs. Time of Flight[5]

The low-thrust trajectory optimization process attempts to limit thrusting to only the most efficient places in the transfer (where the instantaneous orbital elements are favorable) while minimizing the initial C_3 yet meeting the flight time restrictions. As flight time is reduced, thrusting must occur in less efficient parts of the transfer, and more energy from the launch vehicle is required. As flight time increases, however, a point is reached where the number of heliocentric revolutions becomes a limiting factor on performance. Increasing the number of heliocentric revolutions offers the optimizer additional places in the trajectory where highly efficient thrusting can occur. The result is an increase in thrusting efficiency, a decrease in the necessary launch C_3, an increase in flight time and a new family of solutions. This new family of trajectories, like the >2 revolution family indicated in Figure 2, will have a higher minimum flight time but offer better performance at flight times above a certain threshold.

Families of low-thrust trajectories are not only differentiated by the number of revolutions of the trajectory; there are several other ways that the cyclic behavior of the planets cause local minima in trajectory optimization. One classic example is launch opportunity (i.e. the trajectories in Figure 2 could be found one synodic period of Earth and Jupiter later with similar performance). In order to distinguish between families of low-thrust trajectories like the ones in Figure 2, we must develop a classification scheme.

TRAJECTORY FAMILY CLASSIFICATION

The low-thrust gravity-assist trajectory families presented in this paper will be categorized by a few key trajectory features about which locally optimal families form: gravity-assist path, number of transfer revolutions, transfer resonance, transfer flight time, and arrival type. Many of these features occur

---

* Reference 5 includes illustrations of the transfer types whose performance is shown in Figure 2 as well as showing the time history of semimajor axis and eccentricity for a sample trajectory. The optimal injection C_3 is also plotted against flight time.

on each leg of the trajectory, where a leg is defined to be a transfer from one planetary encounter to another. Because of this, each additional flyby body multiplies the number of potential solution families. One type of local minima that will not be included is that associated with the launch opportunity. This type has been omitted because all of the trajectories presented in this paper launch in either 2011 or 2012 so for families that happen to have multiple instances within that time span, the difference in performance will be small. However, if one were comparing the performance of the same trajectory families across many different launch years, it would become an important category.

Path Abbreviation

The first letters of each of the planetary bodies will be listed in the order of encounter to denote the gravity-assist combination or path (note that "M" denotes Mars rather than Mercury). For example, a "VE" trajectory is one that departs from Earth, performs a gravity assist at Venus, then performs a gravity assist at Earth, and arrives at Jupiter. The first and last bodies are not included in the abbreviation because the trajectories presented here will always start at Earth and end at Jupiter.

Number of Revolutions/Transfer Type

As illustrated for the direct cases in Figure 2, differences in the number of heliocentric revolutions for low-thrust trajectories create locally optimal families of solutions in flight time. This occurs on a per-leg basis and so each leg that spans two different bodies must be identified by the angular distance the spacecraft travels about the Sun. However, since the number of revolutions changes as flight time and phasing changes, this category will often be identified by a range.

A trajectory leg is a Type 1 transfer if it travels between 0 and 180 degrees about the Sun. A Type 2 transfer travels between 180 and 360 degrees and the trend continues for Types 3, 4, etc. in increments of 180 degrees. For brevity, type numbers will be indicated with Roman numerals.

Families of trajectories will often have legs that span two different transfer types depending on flight time and phasing, resulting in the need to categorize these trajectories using multiple types. For example, a trajectory leg that travels 160 degrees at one flight time and 200 degrees at another flight time would be a I-II transfer, since it is a I transfer at some flight times and a II at others.

In each of the gravity-assist cases, the transfer from the final flyby to Jupiter rendezvous is a I-II transfer. Other types of gravity assists certainly exist in which the spacecraft would perform multiple revolutions about the Sun before arriving at Jupiter, but these cases have an inherently long flight time so they are not included in this study. Since the transfer type of the last leg of all of the cases presented here is the same, it will not be included in the identification of the trajectory family in an effort to keep the identifiers as short as possible.

Indicating the transfer type is convenient for higher velocity legs that transfer quickly from one body to another, but it becomes inconvenient when describing trajectories with many spirals. An alternative to using the Type number of the transfer is to simply indicate the minimum number of revolutions of the transfer (as in Figure 2).

Resonance

For transfers that return to the same body, the optimizer will avoid extensive and inefficient periapsis rotations by timing the transfer period such that it is approximately resonant with the planet's period. However, since associated with each resonance there is a local minimum, it is important that we record the transfer resonance.[†] Resonance will be indicated by both the number of revolutions the spacecraft performs during the transfer as well as the number of revolutions of the planet.

The flight time for the leg changes as flight time for the entire trajectory changes, so the resonance used to classify each trajectory type will be approximate. Leg resonance will be indicated in the following manner:

[†] An illustration of the local minima associated with resonant transfers can be found in Reference 6. The example case shows two optimal transfers for an Earth gravity assist with different transfer resonances.

Approximate Number of Planet Revolutions : *Approximate Number of Spacecraft Revolutions*

For example, a trajectory leg that starts at Earth and performs one heliocentric revolution before returning to an Earth flyby approximately 2 years later will be referred to as a 2:1 transfer. It should be noted that since these trajectories include thrusting on the transfer, the spacecraft is not necessarily ever in an instantaneous orbit that corresponds to the resonance by which the trajectory is categorized.[‡] This nomenclature is merely a method of indicating the length of the transfer and the number of heliocentric revolutions the spacecraft accomplished.

Transfer Flight Time

The local minima associated with this category are also caused by the periodic motion of the planets. This case, however, is specific to transfers that occur between two different bodies rather than returning to the same body, so the transfer period is no longer in resonance with the planet period. As a result, the optimizer may converge on multiple solutions that perform the same number of heliocentric revolutions but differ in flight times by an integer number of planet revolutions.

As with the resonance cases, it is important to keep track of both the number of spacecraft revolutions and the number of planet revolutions. However, the optimization minima occur at flight times that differ by the period of either (or both) bodies. An illustration of three optimal Venus gravity-assist trajectories with different Earth-Venus transfer times but the same number of spacecraft revolutions is shown in Figure 3. In the leftmost trajectory, the transfer takes 618 days. In the middle trajectory, the Earth departure is approximately one year earlier and the transfer time has been increased by roughly one Earth period. In the rightmost trajectory, the arrival at Venus is approximately one Venus period later, hence the transfer time has been increased by roughly one Venus period. The changes to the flight times are not exact multiples of planetary periods because the flyby conditions change with the increased apoapsis, and because Jupiter is not in the same place when the flyby date changes significantly.

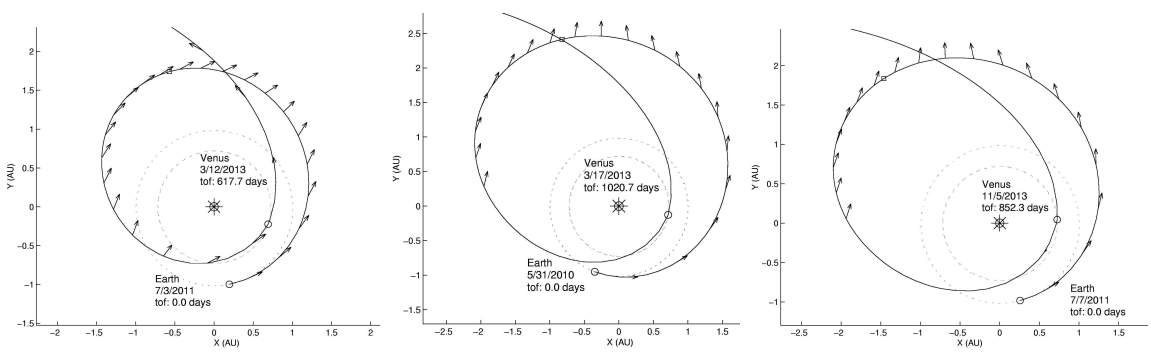

Figure 3 Locally optimal Venus gravity-assist trajectories to Jupiter with different transfer times. The first case (left) has a 618 day transfer. The second case (middle) is the result of departing the Earth approximately one year earlier. The last case (right) is the result of arriving at Venus approximately one Venus year later.

To capture the differences in transfer times between two different bodies, the flight time for the leg will be expressed in number of *whole* revolutions of the *arrival* planet. Unlike the resonance cases, this flight time may need to be expressed as a range for some trajectory families since the transfer time will vary with changes in the total trajectory flight time. Using the three trajectories from Figure 3 as examples for the categorization scheme, the transfer flight time categorization for the first case would be 2 since the transfer time is 618 days (2.75 Venus periods). The transfer time categorization for the second case would be 4 since the transfer time is 1021 days (4.54 Venus periods), and 3 for the last case since the transfer time is 852 days (3.79 Venus periods). At different flight times to Jupiter the Earth-Venus transfer for this last

[‡] An illustration is provided in Reference 6 for a 3:2 resonant Earth gravity-assist case.

case might exceed 900 days in which case the transfer time categorization for the third case would be 3-4. It should also be noted that the second case is different from the others in that it launches in the previous year (2010). This is important to take into account since there is likely a Venus gravity-assist trajectory with an Earth-Venus transfer of the same type that launches in 2011 (the result of shifting the flyby date of the first case forward by two Venus periods).

Arrival Type

By reducing the transfer periapsis below the orbital radius of the target planet, the optimizer can increase the flyby V_∞ and improve the effectiveness of the gravity assist; this technique is known as V_∞ leveraging[8]. When this occurs, there are two points at which the transfer orbit crosses the target planet orbit. The spacecraft can encounter the planet at either of those points as shown in the two trajectories in Figure 4. Because the periapsis is below the target planet, there are two local points of maximum effectiveness for the flyby and as such, optimization minima form. Trajectory legs with flybys that occur prior to perihelion of the transfer are referred to here as inbound; legs with flybys that occur after the transfer perihelion are referred to as outbound.

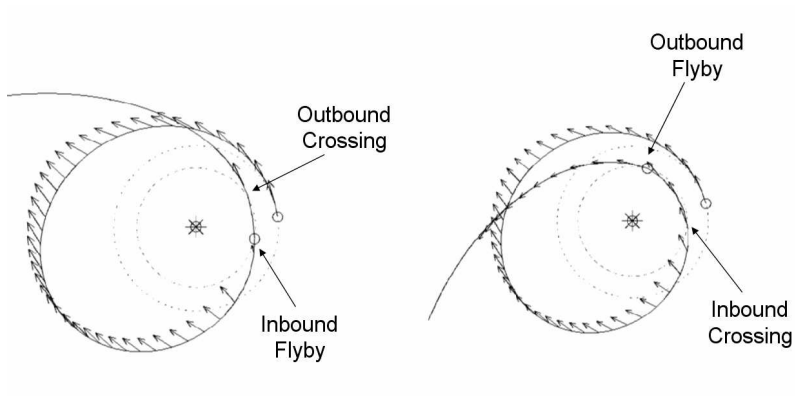

Figure 4 Inbound vs. outbound arrival types. The trajectory on the left is an example of an optimal Venus gravity assist that uses an inbound flyby. The right trajectory is an example of a similar Venus gravity assist with the same transfer type but with an outbound Venus encounter.

For transfers that require significant inclination change, a point of maximum effectiveness for the transfer can occur for transfers both above and below the plane of the ecliptic. As a result, legs with a substantial inclination must also be categorized by whether the arrival at the flyby occurs above or below the plane. For some cases, such as the 0.5:0.5 Earth-Earth transfer, the resonance is exact (a reduction in periapsis for V_∞ leveraging would prevent the orbits from intersecting) and so the above/below plane descriptor is all that is needed to characterize the arrival type for that leg. For other cases, there is not a significant out-of-plane component in which case the inbound or outbound arrival type is all that is needed.

Nomenclature

Locally optimal families of low-thrust gravity assists will be labeled by each of the five previously mentioned categories. The general form is as follows:

Path Abbreviation (T1 A1, T2 A2, etc.)

where

Path Abbreviation:	The first letter of each body in order of encounter
T1:	*Transfer Flight Time* / *Transfer Type* for the first leg if the leg occurs between two different bodies, or *Transfer Resonance* of the first leg if the leg returns to the same body.
A1:	*Arrival type* for the first leg
T2:	*Transfer Flight Time / Transfer Type* or *Transfer Resonance* for the second leg
A2:	*Arrival type* for the second leg

where

Transfer Flight Time:	Leg flight time in number of whole periods of the arrival body
Transfer Type:	"I" if the transfer travels 0-180° about the Sun, "II" for 180-360°, etc.
Transfer Resonance:	*Number of planet revolutions* : *Number of spacecraft revolutions*
Arrival Type:	Inbound (i) if the flyby occurs prior to perihelion of the transfer Outbound (o) if the flyby occurs after perihelion of the transfer Above plane (a) if the transfer is above the plane of the ecliptic Below plane (b) if the transfer is below the plane of the ecliptic

For example, a gravity-assist trajectory family whose first leg is characterized by a I or II transfer (depending on flight time) that required less than 1 Venus period to arrive at an inbound arrival at the Venus flyby, and whose second leg is characterized by a near 2:1 resonant transfer to an outbound arrival at the Venus flyby would be denoted VV (0/I-IIi, 2:1o). Information about the Venus-Jupiter leg has been omitted since all of the combinations presented here end with a I-II transfer to Jupiter rendezvous, similarly the fact that this trajectory launches in 2012 has been omitted. However, this nomenclature could be expanded to include the omitted information by classifying the trajectory EVVJ 2012 (0/I-IIi, 2:1o, I-II).

VEGA FAMILIES

Three families of VEGA trajectories to Jupiter rendezvous are presented here. VEGAs are efficient geometrically due to short transfer times on both the Earth-Venus and Venus-Earth legs. This short transfer time coupled with gravity assists at two massive planets close to the Sun results in a trajectory that performs quite well, even at low flight times.

The shortest flight time VEGA trajectory included here is illustrated in Figure 5 and categorized as VE (0/I-IIo, 0/IIi). The trajectory launches with a positive C_3 (4.84 km^2/s^2) in 2012 and immediately begins using the low-thrust propulsion system to augment the energy supplied by the launch vehicle. This is done because low-thrust propulsion is so much more efficient than the propulsion performed by the launch vehicle. Some launch C_3 is needed however, since this VEGA family has less than one revolution to fly by Venus. Perihelion is reduced below Venus's orbital radius to increase the V_∞. The Venus flyby is outbound since it occurs after the transfer periapsis occurs, and the Venus flyby sets up a Venus-Earth transfer that requires less than one Earth period to return to Earth. The Earth arrival type is inbound to set up the Earth-Jupiter transfer. This trajectory has a substantial amount of thrusting immediately after launch to set up the Venus flyby. More thrusting is later used both before and after the Earth flyby to increase aphelion. Finally, not shown in Figure 5, thrusting occurs at Jupiter to achieve rendezvous.

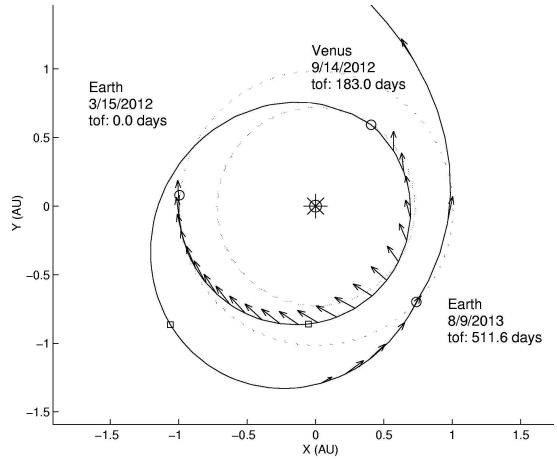

Figure 5 VE (0/I-IIo, 0/IIi) Family Trajectory Plot at 5.4 yrs flight time

The next VEGA trajectory family, shown in Figure 6, is classified as a VE (1-2/III-IVi, 0/IIi). In this case both flybys are inbound, and the first trajectory leg has a longer flight time than the previous case due to an additional revolution. The additional revolution following launch allows the low-thrust propulsion system more time to augment the launch V_∞, thereby reducing the necessary launch energy (to a C_3 of 1 km^2/s^2). This reduction in launch C_3 corresponds to an increase in initial mass which improves the mass at Jupiter rendezvous. However, since the spacecraft must travel around the Sun one additional time, the minimum flight time for this case will be higher than the previous family.

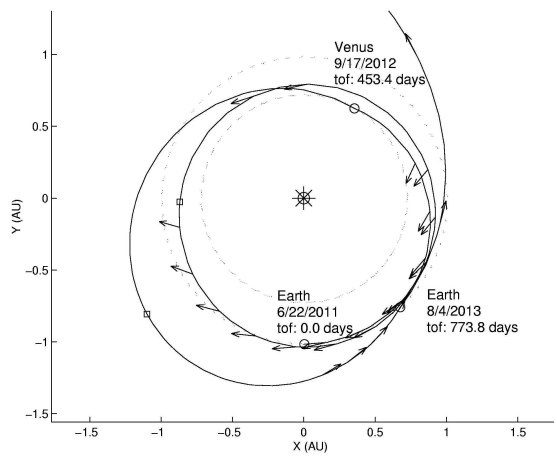

Figure 6 VE (1-2/III-IVi, 0/IIi) Family Trajectory Plot at 6 yrs flight time

The final VEGA case presented, shown in Figure 7, is categorized as a VE (2-3/V-VIi, 1/IIi). Again both flybys are inbound but the first leg of the trajectory has yet another revolution about the Sun. The addition of this revolution allows the thrust arcs to be placed more efficiently, decreasing the propellant mass, while maintaining the low launch C_3 (at 1 km^2/s^2).

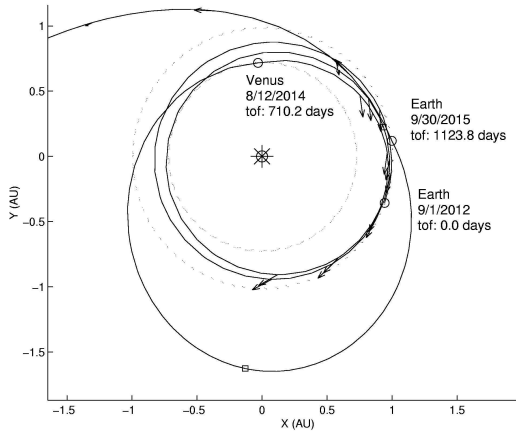

Figure 7 VE (2-3/V-VIi , 1/IIi) Family Trajectory Plot at 6.6 yrs flight time

Another benefit from additional heliocentric revolutions on the first leg of the trajectory is a reduction in sensitivity to phasing. This corresponds to a decrease in performance sensitivity to launch opportunity and an increase in the number of launch opportunities available.

While each of these VEGA families do not occur each year, at least one type is likely to be available on any given year. Either the VE (1-2/III-IVi, 0/IIi) or the VE (0/I-IIo, 0/IIi) was available on each launch year considered (2010-2018). The frequency of the VE (2-3/V-VIi, 1/IIi) was not investigated.

RESULTS

The determination of which gravity-assist trajectory family offers the maximum mass at Jupiter rendezvous is dependant on the maximum allowable flight time, or conversely, the trajectory family that offers the minimum flight time is dependant on the minimum allowable mass at Jupiter rendezvous. The VEGA families illustrated perform quite well when compared to other gravity-assist families. First, we will examine the three VEGA families with respect to each other. Then we will compare them with other gravity-assist paths.

VEGA Performance

The trade between mass and flight time for the three VEGA families presented is shown in Figure 8 with the direct cases shown in Figure 2 as a comparison. All three VEGA families offer substantially greater mass at Jupiter capture than the direct case; however, it is interesting to note that at the higher flight times the advantage of the gravity-assist families over the direct cases is not as great.

By comparing the three VEGA families, it is apparent that additional revolutions on the first leg of the trajectory increase the mass delivered to Jupiter capture at the cost of flight time. The highest delivered mass for the VE (1-2/III-IVi, 0/IIi) family is 4.5% higher than the VE (0/I-IIo, 0/IIi) family, at the cost of an 18% increase in flight time. Similarly, the highest delivered mass for the VE (2-3/V-VIi, 1/IIi) trajectories is 7% higher than the VE (0/I-IIo, 0/IIi) family, at the cost of a 40% increase in flight time. As additional revolutions are added, the flight time increases by roughly the same amount, but the mass gained diminishes.

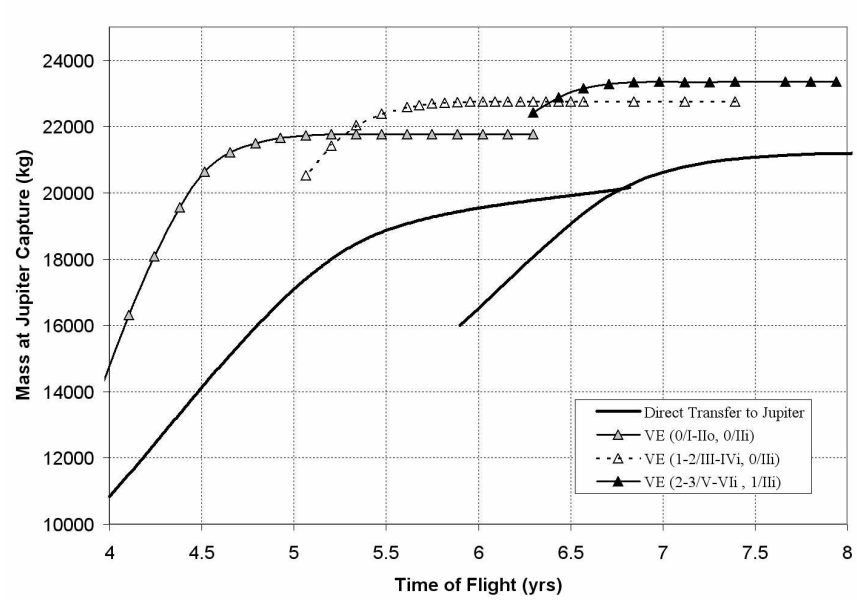

Figure 8 VEGA Performance, Mass at Jupiter Capture vs. Flight Time

The cause of both the performance benefits and the diminishing returns of additional heliocentric revolutions on the first leg of the VEGA trajectories can be seen in Figure 9, which shows the corresponding initial C_3 of the trajectories plotted in Figure 8. The initial C_3 of the VE (0/I-IIo, 0/IIi) family is significantly higher than the other two families due to the geometry of the Earth-Venus transfer. However, as additional heliocentric revolutions are added to the first leg of the transfer, the C_3 reaches very low values. With enough revolutions prior to the first flyby, the mass gained by adding additional revolutions is insignificant.

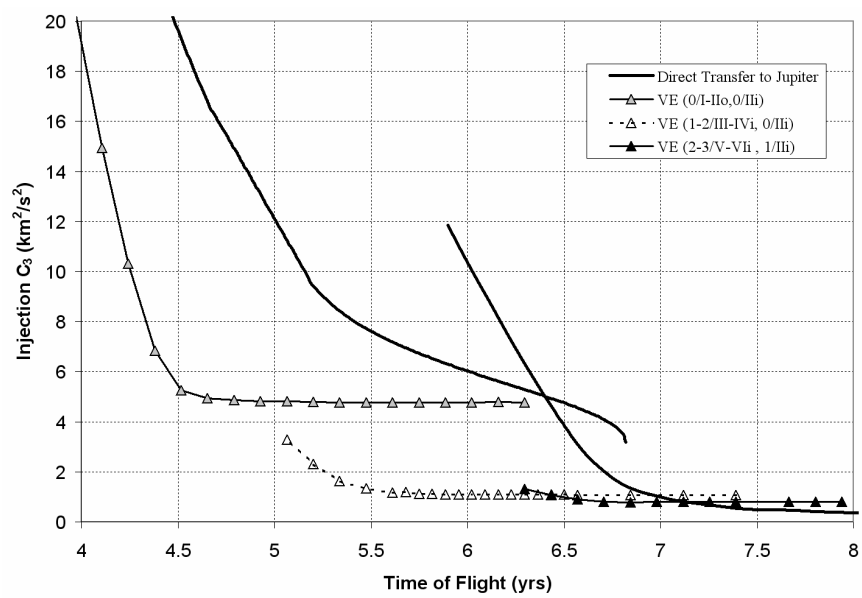

Figure 9 VEGA Performance, Injection C_3 vs. Flight Time

The total low-thrust ΔV for the trajectories in Figure 8 is shown in Figure 10. There are two major factors influencing the ΔV for these transfers. One is the launch C_3; an increase in launch C_3 means that the

low-thrust propulsion system is required to perform less of the total ΔV needed. The second major influence to the low-thrust ΔV is the effectiveness of the thrusting. As additional heliocentric revolutions are added thrusting becomes more efficient as it is centered about the most effective places in the transfer to thrust. The VE (0/I-IIo, 0/IIi) family has the lowest low-thrust ΔV due to the fact that the launch vehicle is supplying much of the energy needed. The VE (1-2/III-IVi, 0/IIi) family requires additional ΔV due to the fact that the low-thrust propulsion system reduces the injection C_3 needed significantly. The VE (2-3/V-VIi, 1/IIi) trajectory also decreases the initial C_3, but the additional revolution allows the optimizer to place thrusting more effectively, thereby enabling it to reduce the total low-thrust ΔV. This effect is also evident when comparing Figure 6 and Figure 7, as the VE (2-3/V-VIi, 1/IIi) trajectory in Figure 7 has shorter, more concentrated thrust arcs. Also note that the "knees" of the curves are offset by roughly one year, approximately the amount of additional flight time required for one revolution on the first leg.

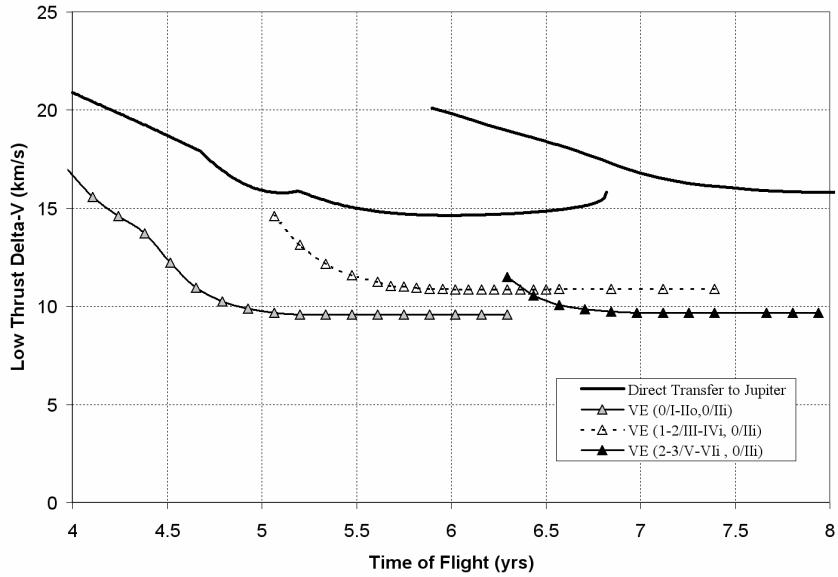

Figure 10 VEGA Performance, ΔV vs. Flight Time

The effect of additional heliocentric revolutions on the first leg of the VEGA trajectories can also be seen on gravity-assist trajectories with different planetary flyby combinations, and while the VEGA trajectories perform quite well in comparison to the direct cases, other planetary gravity-assist combinations are able to offer similar or better performance.

Gravity-Assist Trajectory Family Comparison

Tables 1-4 list information about each of 35 different trajectory families for 8, 7, 6 and 5 year flight times respectively, all launching in either 2011 or 2012. The trajectory families in each table are in order of mass at Jupiter rendezvous starting with the largest delivered mass for the given flight time. Some trajectory families are indicated as not having data at certain flight times. This occurs either because the family has a short flight time and the delivered mass has reached a maximum, in which case the higher flight times were not pursued, or the family has a longer flight time, in which case the trajectory would not converge for flight very low flight times. Figure 11 is a plot of the performance of all of the trajectory families against flight time.[§]

[§] None of the trajectories presented in this paper have constraints on the declination of the launch asymptote (DLA). The 0.5:0.5 resonant EEGA cases optimize to values of DLA that no longer correspond to the launch vehicle curve presented earlier. The result is a relative increase in performance for these cases with respect to the others. However, even with this unfair advantage, the 0.5:0.5 EEGA cases perform poorly with respect to other trajectory types.

Table 1 Gravity-Assist Trajectory Family Performance, 8 year flight time

Trajectory Type	Launch Date (yy/mm/dd)	Flight Time to Flybys ($1^{st}/2^{nd}/3^{rd}$)	Mass at Jupiter (kg)	Low-thrust ΔV (km/s)	Launch C_3 (km^2/s^2)
EE (1:1o, 2:1i)	11/08/22	464 / 1146	24030	8.48	0.32
EE (2:2i, 2:1i)	12/11/08	802 / 1491	24009	8.48	0.37
EE (1:1o, 2:1o)	11/05/26	466 / 1243	23990	8.55	0.35
EE (1:1i, 2:1i)	11/09/01	446 / 1133	23886	8.74	0.41
EE (1:1i, 2:1o)	12/07/14	444 / 1230	23802	8.91	0.45
EE (1.5:1.5i, 2:1i)	12/04/04	623 / 1313	23791	9.30	0.10
VE (2-3/V-VIi , 1/IIi)	12/08/14	730 / 1148	23350	9.67	0.80
E (4:3i)	11/12/17	1411	22921	10.87	0.70
E (4:3o)	11/08/26	1557	22900	10.96	0.66
EE (1:1i, 3:1i)	11/09/03	447 / 1540	22859	11.03	0.69
VE (1-2/III-IVi, 0/IIi)	11/06/21	454 / 775	22764	10.87	1.08
E (2:2o)	12/07/16	812	22537	12.33	0.25
EE (0.5:0.5a, 3:2o)	12/03/01	195 / 1370	22367	11.43	1.53
M (0/III-IVo)	11/04/11	596	22271	12.91	0.36
E (2:2i)	12/05/10	825	22227	12.82	0.56
E (3:2o)	11/07/21	1198	22154	11.35	2.15
E (3:2i)	11/10/27	1070	22052	11.18	2.57
VE (0/I-IIo, 0/IIi)	12/03/15	183 /512	21776	9.58	4.78
E (3.5:2.5i)	12/04/03	1295	21731	14.08	0.62
M (0/I-IIo)	11/10/08	328	21723	11.57	3.04
VEE (0/I-IIo, 1/II-IIIo, 2:1i)	12/03/21	180 / 704 / 1298	21292	10.16	5.48
EE (0.5:0.5a, 1:1i)	11/10/05	195 / 611	21274	15.13	0.81
Direct >2 Revolutions**	--	--	21193	15.82	0.37
VV (1-2/III-IVo, 2:1i)	11/04/20	467 / 941	20867	13.65	3.31
V (3-4/IV-Vi)	11/09/30	979	20702	15.04	2.44
EE (0.5:0.5a, 2:1i)	12/04/27	188 / 892	20685	10.55	6.71
VV (0/I-IIi, 2:1o)	12/03/07	118 / 603	20276	10.51	7.85
E (2:1i)	12/10/15	718	19230	10.54	10.70
E (2:1o)	12/07/20	833	18815	10.85	11.59
V (2/II-IIIi)	11/07/02	618	18424	13.51	10.29
E (1:1o)	--	--	--	--	--
E (1:1i)	--	--	--	--	--
E (1.5:1.5o)	--	--	--	--	--
E (1.5:1.5i)	--	--	--	--	--

** Launch and arrival dates are not listed for the direct trajectory families because the ephemeris for Earth and Jupiter was not used to generate those results. Instead, the direct trajectory results were generated using circular, coplanar orbits of Earth and Jupiter. This was done to allow the direct transfer results to be general in terms of launch opportunity. The circular, coplanar simplifying assumption was not used for the gravity-assist results since performance can depend significantly on injection opportunity.

Table 2 Gravity-Assist Trajectory Family Performance, 7 year flight time

Trajectory Type	Launch Date (yy/mm/dd)	Flight Time to Flybys ($1^{st}/2^{nd}/3^{rd}$)	Mass at Jupiter (kg)	Low-thrust ΔV (km/s)	Launch C_3 (km^2/s^2)
EE (1:1o, 2:1i)	11/08/22	463 / 1146	24029	8.49	0.32
EE (1:1o, 2:1o)	11/06/09	453 / 1229	23942	8.61	0.40
EE (1:1i, 2:1i)	11/09/01	445 / 1133	23885	8.74	0.41
EE (1:1i, 2:1o)	12/07/17	438 / 1224	23767	9.00	0.45
EE (1.5:1.5i, 2:1i)	12/05/19	573 / 1263	23595	9.81	0.07
VE (2-3/V-VIi , 1/IIi)	12/08/14	731 / 1148	23349	9.66	0.81
VE (1-2/III-IVi, 0/IIi)	11/06/21	454 / 775	22764	10.87	1.08
E (2:2o)	12/07/16	812	22538	12.32	0.25
M (0/III-IVo)	11/04/12	596	22273	12.90	0.37
E (2:2i)	12/05/13	827	22212	12.82	0.60
E (3:2o)	11/07/23	1196	22152	11.35	2.15
E (4:3i)	12/02/25	1333	22126	12.86	0.78
EE (0.5:0.5a, 3:2o)	12/03/31	187 / 1336	22072	11.55	2.17
E (3:2i)	11/10/26	1071	22050	11.19	2.56
VE (0/I-IIo, 0/IIi)	12/03/15	183 / 512	21776	9.58	4.78
E (3.5:2.5i)	12/04/03	1295	21731	14.08	0.62
M (0/I-IIo)	11/10/08	327	21722	11.57	3.04
VEE (0/I-IIo, 1/II-IIIo, 2:1i)	12/03/22	179 / 698 / 1289	21147	10.50	5.54
EE (0.5:0.5a, 1:1i)	11/11/05	189 / 599	20994	14.87	1.81
VV (1-2/III-IVo, 2:1i)	11/04/20	467 / 941	20867	13.65	3.31
V (3-4/IV-Vi)	11/09/30	979	20702	15.04	2.44
EE (0.5:0.5a, 2:1i)	12/04/26	188 / 893	20684	10.55	6.72
Direct >2 Revolutions	--	--	20616	16.80	0.99
VV (0/I-IIi, 2:1o)	12/03/07	118 / 603	20275	10.52	7.84
EE (1:1i, 3:1i)	11/12/07	343 / 1432	19951	14.57	4.94
E (2:1i)	12/10/15	718	19230	10.54	10.70
E (2:1o)	12/07/20	833	18815	10.85	11.59
V (2/II-IIIi)	11/07/02	618	18424	13.51	10.29
E (1:1o)	--	--	--	--	--
E (1:1i)	--	--	--	--	--
E (1.5:1.5o)	--	--	--	--	--
E (1.5:1.5i)	--	--	--	--	--
EE (2:2i, 2:1i)	--	--	--	--	--
E (4:3o)	--	--	--	--	--

Table 3 Gravity-Assist Trajectory Family Performance, 6 year flight time

Trajectory Type	Launch Date (yy/mm/dd)	Flight Time to Flybys (days) ($1^{st}/2^{nd}/3^{rd}$)	Mass at Jupiter (kg)	Low-thrust ΔV (km/s)	Launch C_3 (km^2/s^2)
VE (1-2/III-IVi, 0/IIi)	11/06/22	453 / 744	22762	10.87	1.09
E (2:2o)	12/07/21	813	22499	12.42	0.26
EE (1:1o, 2:1i)	11/11/30	353 / 1033	22245	11.35	1.92
EE (1:1i, 2:1i)	11/12/08	337 / 1021	22161	11.95	1.56
M (0/III-IVo)	11/05/09	580	22147	12.87	0.72
E (1.5:1.5o)	12/01/09	589	22118	13.22	0.45
E (2:2i)	12/05/31	820	21979	13.26	0.77
VE (0/I-IIo, 0/IIi)	12/03/15	183 / 512	21776	9.59	4.78
M (0/I-IIo)	11/10/07	333	21611	11.87	3.04
E (3:2i)	11/12/01	1024	21303	12.22	3.51
VV (1-2/III-IVo, 2:1i)	11/04/16	467 / 940	20734	13.53	3.78
EE (1:1o, 2:1o)	11/11/03	331 / 1086	20730	13.95	3.40
E (1.5:1.5i)	12/03/17	474	20695	14.12	3.33
EE (0.5:0.5a, 2:1i)	12/04/24	189 / 892	20652	10.58	6.77
E (1:1i)	12/05/12	415	20613	13.90	3.76
V (3-4/IV-Vi)	11/10/03	973	20589	15.21	2.57
EE (0.5:0.5a, 1:1i)	11/11/23	187 / 593	20537	14.94	2.98
EE (1:1i, 2:1o)	12/12/04	314 / 1084	20358	14.82	3.57
VV (0/I-IIi, 2:1o)	12/03/07	118 / 603	20274	10.54	7.82
E (3:2o)	11/10/27	1091	20078	15.27	3.93
Direct >1 Revolution	--	--	19538	14.6	6.03
E (2:1i)	12/10/15	718	19230	10.56	10.69
E (2:1o)	12/07/20	833	18815	10.86	11.58
V (2/II-IIIi)	11/07/02	618	18424	13.51	10.29
EE (0.5:0.5a, 3:2o)	12/08/28	166 / 1180	15913	21.14	11.20
VEE (0/I-IIo, 1/II-IIIo, 2:1i)	12/04/22	151 / 646 / 1160	15659	22.55	10.77
EE (1:1i, 3:1i)	11/12/20	284 / 1262	11548	26.23	23.40
E (1:1o)	--	--	--	--	--
E (4:3i)	--	--	--	--	--
E (4:3o)	--	--	--	--	--
E (3.5:2.5i)	--	--	--	--	--
EE (1.5:1.5i, 2:1i)	--	--	--	--	--
EE (2:2i, 2:1i)	--	--	--	--	--
VE (2-3/V-VIi, 1/IIi)	--	--	--	--	--

Table 4 Gravity-Assist Trajectory Family Performance, 5 year flight time

Trajectory Type	Launch Date (yy/mm/dd)	Flight Time from Launch to Flybys ($1^{st}/2^{nd}/3^{rd}$)	Mass at Jupiter (kg)	Low-thrust ΔV (km/s)	Launch C_3 (km^2/s^2)
VE (0/I-IIo, 0/IIi)	12/03/15	182 / 510	21730	9.67	4.82
E (1.5:1.5o)	12/03/17	534	21705	12.95	1.78
E (1:1o)	12/07/02	417	21358	12.80	2.81
E (2:2o)	12/12/11	667	20913	14.88	2.02
M (0/III-IVo)	11/07/12	542	20729	14.01	3.34
VE (1-2/III-IVi, 0/IIi)	11/08/26	388 / 700	20535	14.61	3.29
VV (0/I-IIi, 2:1o)	12/03/08	118 / 604	20253	10.59	7.83
M (0/I-IIo)	11/10/23	331	19979	14.39	5.03
E (1:1i)	12/06/01	408	19858	13.88	5.85
E (1.5:1.5i)	12/03/27	476	19754	14.52	5.53
EE (0.5:0.5a, 1:1i)	11/12/12	185 / 582	19148	15.77	6.08
E (2:1i)	12/10/16	708	18801	11.17	11.35
V (2/II-IIIi)	11/07/02	618	18419	13.45	10.36
E (2:2i)	12/10/01	692	18108	17.18	7.83
E (2:1o)	12/08/22	791	17628	12.65	13.45
Direct >1 Revolution	--	--	17094	15.92	12.12
VV (1-2/III-IVo, 2:1i)	11/07/06	387 / 852	16322	18.54	12.22
EE (0.5:0.5a, 2:1i)	12/06/14	178 / 807	16273	16.65	14.09
V (3-4/IV-Vi)	12/01/20	861	14688	20.55	16.00
E (3:2i)	12/05/02	872	13616	20.73	19.79
E (3:2o)	--	--	--	--	--
E (3.5:2.5i)	--	--	--	--	--
E (4:3i)	--	--	--	--	--
E (4:3o)	--	--	--	--	--
EE (0.5:0.5a, 3:2o)	--	--	--	--	--
EE (1:1o, 2:1i)	--	--	--	--	--
EE (1:1o, 2:1o)	--	--	--	--	--
EE (1:1i, 2:1o)	--	--	--	--	--
EE (1:1i, 2:1i)	--	--	--	--	--
EE (1:1i, 3:1i)	--	--	--	--	--
EE (1.5:1.5i, 2:1i)	--	--	--	--	--
EE (2:2i, 2:1i)	--	--	--	--	--
VE (2-3/V-VIi, 1/IIi)	--	--	--	--	--
VEE (0/I-IIo, 1/II-IIIo, 2:1i)	--	--	--	--	--

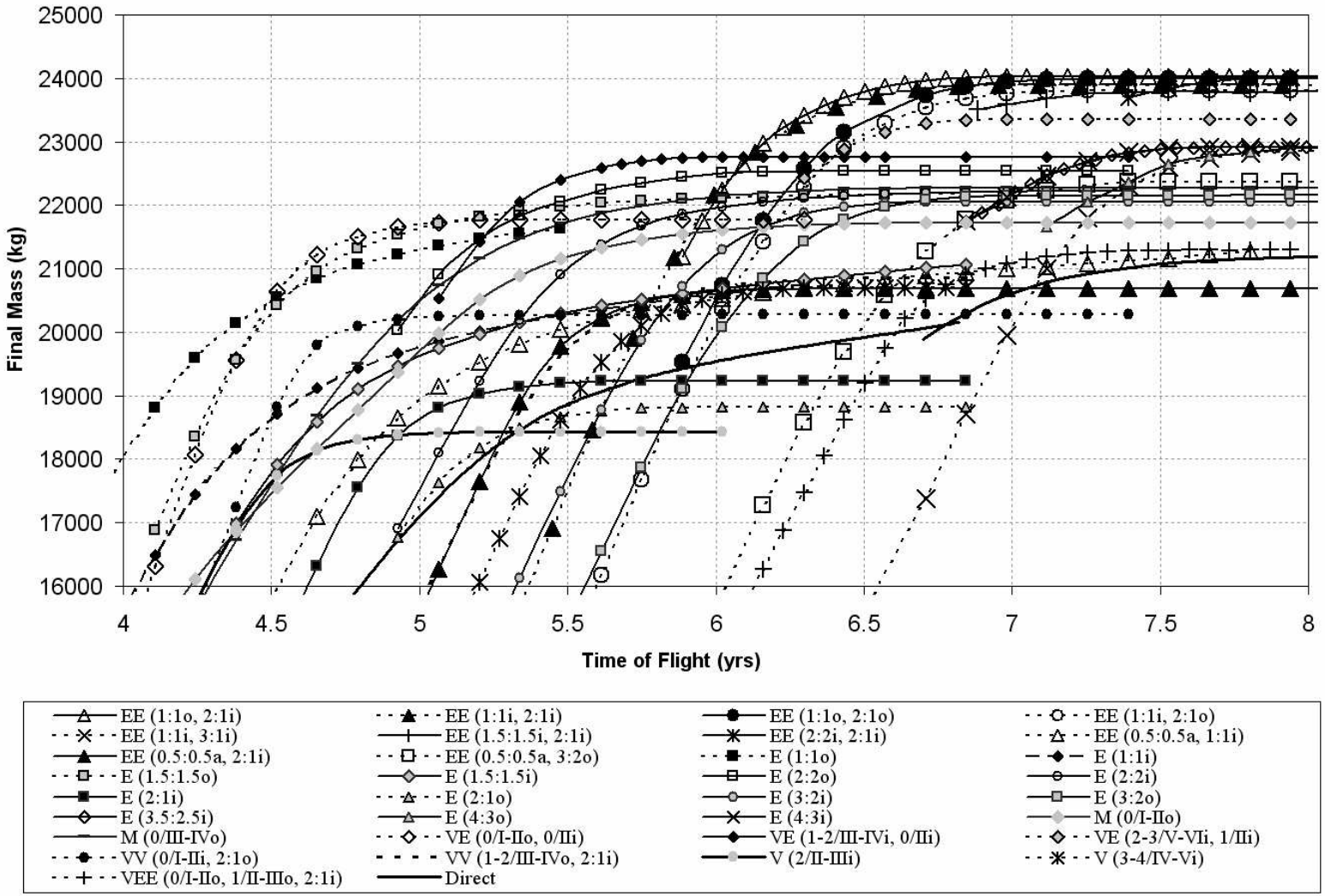

Figure 11 Gravity-Assist Combination Parametrics

At an 8 year flight time to Jupiter, Table 1 shows that the top 6 trajectories in terms of mass delivered to Jupiter are all double Earth gravity-assist cases. These EE cases perform well due to their low initial C_3 and two flybys. The VE (2-3/V-VIi , 1/IIi), E (4:3i), and E (4:3o) cases are also able to maintain low initial C_3 values to achieve high delivered masses. It is interesting to note that the top 10 gravity-assist cases in this table all have optimal C_3 values of less than 1, but that none of the cases in any of the four tables have a zero value for launch C_3, indicating that there is almost always a benefit to a small initial C_3.

At a 5 year flight time, only 20 of the 35 total trajectory families had solutions (as opposed to 30 at an 8 year flight time). At that flight time, the VE (0/I-IIo, 0/IIi) family outperforms the other trajectory families, as it benefits from two gravity assists in only 510 days. The EE (0.5:0.5a, 1:1i) family performs two gravity assists in less than 600 days, but the performance suffers due to a high initial C_3 requirement for the initial 0.5:0.5 transfer. Other trajectory families that perform well at 5 years flight time are the single Earth gravity assists that use an outbound flyby and a low initial resonance to keep C_3 low, and the M (0/III-IVo) family which uses a low initial C_3 and spirals to a Mars flyby. At low flight times, the top performing trajectories are those that require a low initial C_3 while maintaining compact geometries such that they require little flight time before performing the final gravity assist.

The Venus-Earth, Earth and Mars gravity-assist families perform consistently well; at least one family from each of those gravity-assist combinations is near the top of the list in terms of performance at each of the flight times examined. The double Earth gravity assists performed very well at high flight times but could not achieve reasonable masses at flight times of lower than about 6 years. The high performance of the Earth, double Earth, and Mars gravity-assist cases for the low-thrust propulsion system contrasts sharply against the impulsive scenario where these three gravity-assist types offer relatively poor performance[9].

As flight time increases, gravity assists offer less and less improvement over direct trajectories. Additional revolutions allow the direct trajectories to reduce C_3 and thrust very efficiently, while the geometry of gravity assists causes them to maintain higher initial C_3's and constrain thrusting. At 8 years flight time, the best direct trajectory offers approximately 88% of the mass that the best gravity-assist case delivers. At 5 years flight time that fraction is reduced to 79% and continues to decrease as flight time is reduced further.

The performance results for the cases shown, both absolute and relative, will change with changes to the propulsion system parameters (ie: launch vehicle, power, Isp, etc.). General trends will remain the same if the acceleration is similar, but the top performers at a given flight time may vary.

CONCLUSIONS

The low-thrust trajectory optimization problem is one with many local minima that occur for a number of reasons. The features about which these local minima form can be used to categorize families of trajectories. These features include the gravity-assist path or combination of planets, the leg transfer type or number of heliocentric revolutions, the leg resonance in cases where resonance occurs, the leg flight time, and each arrival type. Additionally, local minima form about each launch opportunity, though the launch opportunities for the trajectories presented here were limited to 2011 or 2012.

Adding heliocentric revolutions to the first leg of a trajectory allows some of the initial energy previously provided by the launch vehicle to be provided by the more efficient low-thrust propulsion. The additional revolutions also allow the low-thrust propulsion to be performed at more efficient places in the transfer. This mass savings comes at the cost of flight time, however, and with diminishing returns as more revolutions are added. This effect was illustrated with the three Venus-Earth gravity-assist families. The Venus-Earth gravity-assist families also illustrate how a higher low-thrust ΔV can result in increased final mass due to a reduction in launch C_3.

While many gravity-assist trajectory families exist with different resonances, or arrival types or numbers of revolutions, it is not possible to find one family that performs best at all flight times. At any one flight time there may be several trajectory families that perform comparably, and selecting between them may be subject to other criteria. Gravity-assist trajectory families that can launch with low injection C_3's are able to launch with greater initial mass than higher initial C_3 cases and, as a result, given sufficient flight time, are able to deliver more final mass. At higher flight times, the top performing Jupiter rendezvous trajectories are from families that start with a low initial C_3 and reduce low-thrust ΔV through

multiple gravity assists and/or more efficient placement of thrusting. The four EE(1:1, 2:1) cases, along with the VE(2-3/V-VIi, 1/IIi), and E(4:3i) cases are able to accomplish this. At lower flight times families like the VE (0/I-IIo, 0/IIi), E (1.5:1.5o), or M (0/III-IVo) are able to capitalize on relatively compact geometries and low initial C_3's to get to Jupiter quickly while still offering good performance. Overall, for low-trust trajectories, gravity assists offer a way to potentially reduce flight time, increase delivered mass, or both.

ACKNOWLEDGEMENTS

The authors would like to thank Paul Finlayson, Ed Rinderle, and Ben Engebreth for their efforts in developing and enhancing the low-thrust trajectory optimization software used to obtain these results. We are also grateful to Louis D'Amario, Anastassios Petropoulos, and Ryan Russell for their insights into impulsive trajectory types. This work was performed at the Jet Propulsion Laboratory, California Institute of Technology, under a contract with the National Aeronautics and Space Administration. The opinions and conclusions expressed in this paper are those of the authors and do not necessarily reflect the policies of the National Aeronautics and Space Administration.

REFERENCES

1. Williams, S. N., and Coverstone-Carroll, V., "Benefits of Solar Electric Propulsion for the Next Generation of Planetary Exploration Missions," *Journal of the Astronautical Sciences*, Vol. 45, No. 2, April-June 1997, pp. 143-159.

2. Sauer, C. G., Jr., and Yen, C. L., "Planetary Mission Capability of Small Low Power Solar Electric Propulsion Systems," IAA-L-0706, IAA International Conference on Low-Cost Planetary Missions, Laurel, MD, April 12-15, 1994.

3. Rayman, M. D., and Lehman, D. H., "NASA's First New Millennium Deep-Space Technology Validation Flight," IAA-L-0502, Second IAA International Conference on Low-Cost Planetary Missions, Laurel, MD, April 16-19, 1996.

4. Yam, C. H., McConaghy, T. T., Chen, K. J., and Longuski, J. M., "Preliminary Design of Nuclear Electric Propulsion Missions to the Outer Planets," AIAA/AAS Astrodynamics Specialist Conference, AIAA Paper 2004-5393, Providence, RI, August 16-19, 2004.

5. Parcher, D. W., and Sims, J. A., "Venus and Mars Gravity-Assist Trajectories to Jupiter Using Nuclear Electric Propulsion," AAS/AIAA Astrodynamics Specialists Conference, AAS Paper 05-112, Copper Mountain, CO, January 23-27, 2005.

6. Parcher, D. W., and Sims, J. A., "Earth Gravity-Assist Trajectories to Jupiter Using Nuclear Electric Propulsion," AAS/AIAA Astrodynamics Specialists Conference, AAS Paper 05-397, Lake Tahoe, CA, August 7-11, 2005.

7. Sims, J. A., and Flanagan, S. N., "Preliminary Design of Low-Thrust Interplanetary Missions," AAS/AIAA Astrodynamics Specialists Conference, AAS Paper 99-338, Girdwood, AK, August 16-19, 1999.

8. Sims, J. A., Longuski, J. M., and Staugler, A. J., "V_∞ Leveraging for Interplanetary Missions: Multiple-Revolution Orbit Techniques," *Journal of Guidance, Control, and Dynamics*, Vol. 20, No. 3, 1997, pp. 409-415.

9. Petropoulos, A. E., Longuski, J. M., and Bonfiglio, E. P., "Trajectories to Jupiter via Gravity Assists from Venus, Earth, and Mars," *Journal of Spacecraft and Rockets*, Vol. 37, No. 6, Neptune-December 2000, pp. 776-783.